Tailored design of an oxygen-rich stable Co-MOF integrated with MXene nanofibers as advanced heterostructures for high-performance ammonium-ion supercapacitors

Nissar Hussain[a] and Shaikh M. Mobin*[, a, b,]

[a] Department of Chemistry, Indian Institute of Technology Indore, Simrol, Khandwa Road, Indore 453552, India.

[b] Centre for Advance Electronics (CAE), Indian Institute of Technology Indore, Simrol, Khandwa Road, Indore 453552, India.

*E-mail: xray@iiti.ac.in

Table of Contents

S. No.	Descriptions	Page No.
1.0	**Material Characterizations**	**S3**
1.1	**X-Ray Structural Studies**	**S3**
2.0	**Electrochemical Measurements**	**S4**
2.1	**Electrochemical Calculations**	**S4**
3.0	**Fig. S1.** a) The asymmetric unit of Co-MOF. b) 2D sheet along c-axis	**S5**
4.0	**Fig. S2.** ATR-FTIR spectrum of Co-MOF and Co-MOF@MXCNF heterostructure.	**S6**
4.1	**Fig. S3.** FE-SEM images of a,b) MXene ($Ti_3C_2T_x$). c,d) Co-MOF at different magnifications respectively.	**S7**
4.2	**Fig. S4.** XPS Survey scan of Co-MOF@MXCNF	**S8**
4.3	**Fig. S5**. XPS of a) Nitrogen (N 1s) b) Carbon (C 1s) c) Oxygen (O 1s)	**S9**
5.0	**Fig. S6**. a) N_2 adsorption and desorption b) BJH pore size distribution of Co-MOF@MXCNF, Co-MOF, and MXCNF respectively.	**S10**
6.0	**Fig. S7.** Comparison of CV curves of Co-MOF and Co-MOF@MXCNF electrodes.	**S11**
6.1	**Fig. S8.** ATR-FTIR spectrum of Co-MOF@MXCNF electrode for initial, charging, and discharging respectively.	**S12**
7.0	**Table S1:** X-ray crystal structure data and refinement parameters of Co-MOF	**S13**
7.1	**Table S2:** Bond Length and Bond Angle for Co-MOF	**S14**
8.0	**Table S3.** Comparison of as-synthesized material with previous reports	**S26**
8.1	**Table S4.** Comparison of as-synthesized material with previous AIHSCs reports	**S27**
9.0	**References**	**S28**

Material Characterizations

The Single crystal data were collected by using Bruker D8 Quest Single Crystal - XRD at 150(2) K using graphite monochromated Mo Kα radiation (λα = 0.71073 Å). For Thermogravimetric analysis (TGA), the Mettler Toledo (TGA/DSC 1) analyzer with STARe software was heated up to 800 °C using a 10 °C/min rate under an N_2 flow. Cu K (0.154 nm) monochromatic radiation was employed with a Rigaku Smart Lab X-ray diffractometer for the Powder X-ray Diffraction (PXRD) investigation. The attenuated total reflectance Fourier transform infrared (ATR-FTIR) spectra were recorded with a Bruker Alpha II system over the wavenumber range of 4000−400 cm^{-1}. The morphology of samples was captured on a Zeiss Supra55 field-emission scanning electron microscope (FE-SEM) images and 300 KV (Tecnai G2 F 30) transmission electron microscope (TEM). Brunauer-Emmett-Teller (BET) surface area of the composite and its Barrett-Joyner-Halenda (BJH) pore size distribution were found out on an Autosorb iQ, (Quantachrome Instruments, version 1.11). using N_2 flow, X-ray photoelectron spectroscopy (XPS) was performed on an XPS spectrometer (PHI 5000 VersaProbe III spectrophotometer (ULVAC-PHI INC), using Al Kα as the X-ray source.

X-Ray Structural Studies

The single-crystal structure of Cu-MOF was produced using a Rigaku Oxford Supernova CCD diffractometer. Single-crystal X-ray diffraction (SCXRD) analysis was conducted at 293 K with monochromatic graphite Cu Kα (1.548 Å), and the collection was determined through *CrysAlisPro CCD* software. Data collection was done with the standard φ–ω scan methods and scaled/reduced with *CrysAlisPro RED* software. The crystal structure was determined through direct techniques with *SHELXS-97* and refined with full-matrix least squares using *SHELXL-97* on F^2.[1] Every atom was located through direct methods, and all non-H elements were obtained anisotropically. All of the H atoms were in geometrically controlled places and refined by isotropic temperature factors that are generally $1.2U_{eq}$ of their parent atoms. The non-covalent electrostatic interaction, mean-plane determination, and molecular diagrams are produced from the *DIAMOND* program, version 3.1d. [2]

Electrochemical measurements

The as-synthesized Co-MOF@MXCNF freestanding electrode was carefully cut into 1 × 1 cm^2 (a mass loading of 3 mg) and was used as a working electrode with Ag/AgCl as a reference electrode, and graphite rod as the counter electrode in three electrodes set up. To determine the electrochemical performance, cyclic voltammetry (CV), galvanostatic charge-discharge (GCD) measurements, and electrochemical impedance spectroscopy (EIS) were carried out on an Autolab workstation using a 2M $(NH_4)_2SO_4$ aqueous solution as an electrolyte. The electrochemical study of control samples i.e., pristine Co-MOF is studied by drop casting MOF on Carbon paper as a working electrode (dispersion in ethanol achieved a mass loading of around 2 mg). The two-electrode system was fabricated using carbon paper as the current collector. As for the electrolytes, PVA–$(NH_4)_2SO_4$ was applied to the electrodes. PVA–KOH gel was coated on the electrode, which was solidified at room temperature. Finally, the assembly of the solid-state supercapacitor demonstrated that the positive electrode and negative electrode were completely separated by cellulose paper and fixed for further use to record the efficiency of the devices.

Electrochemical Calculations

The areal capacitances (C_s, $F\ g^{-1}$) were calculated based on the GCD curves according to the following equation (1):

$$C_s = \frac{I\Delta t}{m\Delta V} \quad \text{.....(1)}$$

where I/m is the current density (A g^{-1}) and t is the discharge time (s). v is the potential window (V).

The areal energy densities (E, $mWh\ Kg^{-1}$) and power densities (P, $mW\ Kg^{-1}$) were calculated from equations (2) and (3):

$$E = \frac{C_S}{2 \times 3.6} \times \Delta V^2 \quad \text{.....(2)}$$

$$P = \frac{E}{\Delta t} \times 3600 \quad \text{.....(3)}$$

where ΔV is the discharge voltage range (V) and Δt is the discharge time (s).

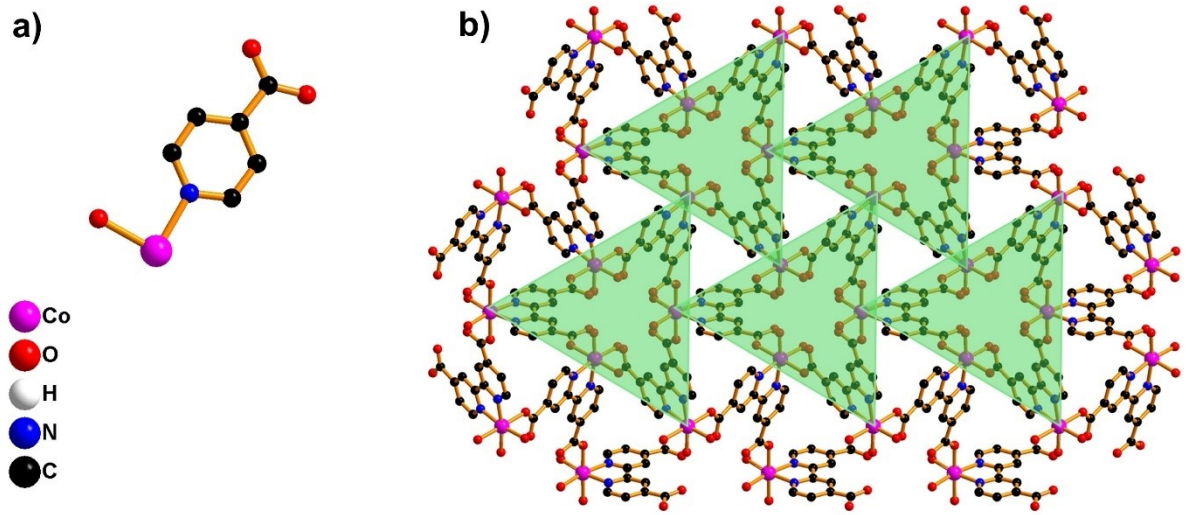

Fig. S1. a) The asymmetric unit of Co-MOF. b) 2D sheet along c-axis

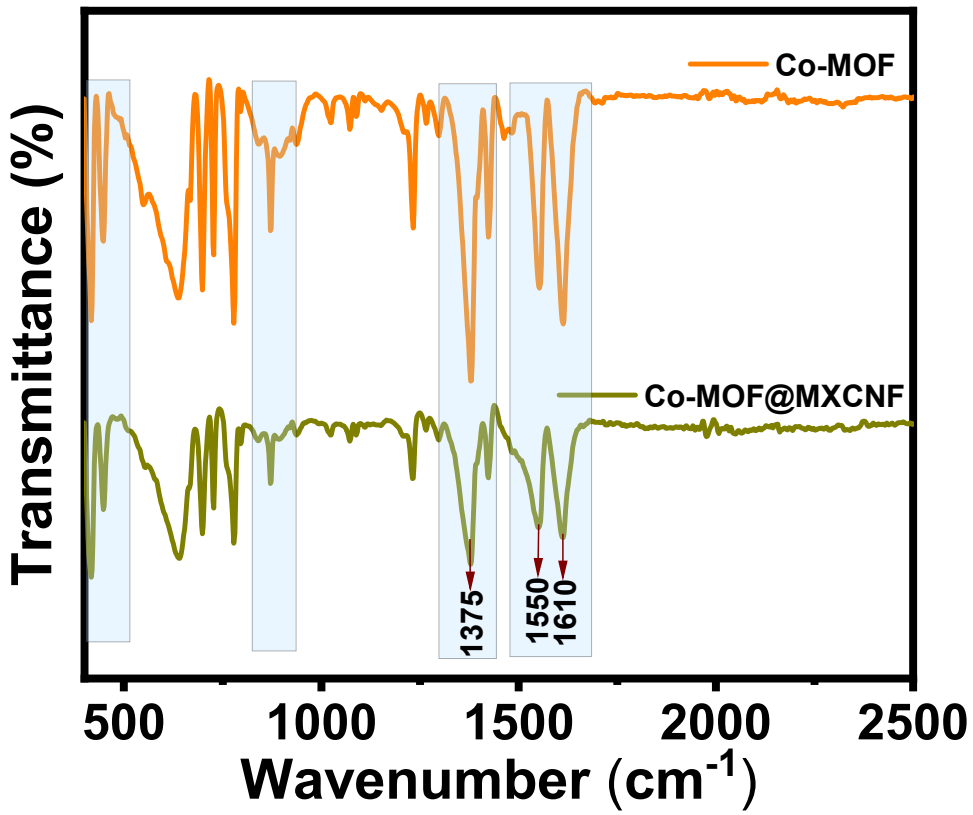

Fig. S2. ATR-FTIR spectrum of Co-MOF and Co-MOF@MXCNF heterostructure.

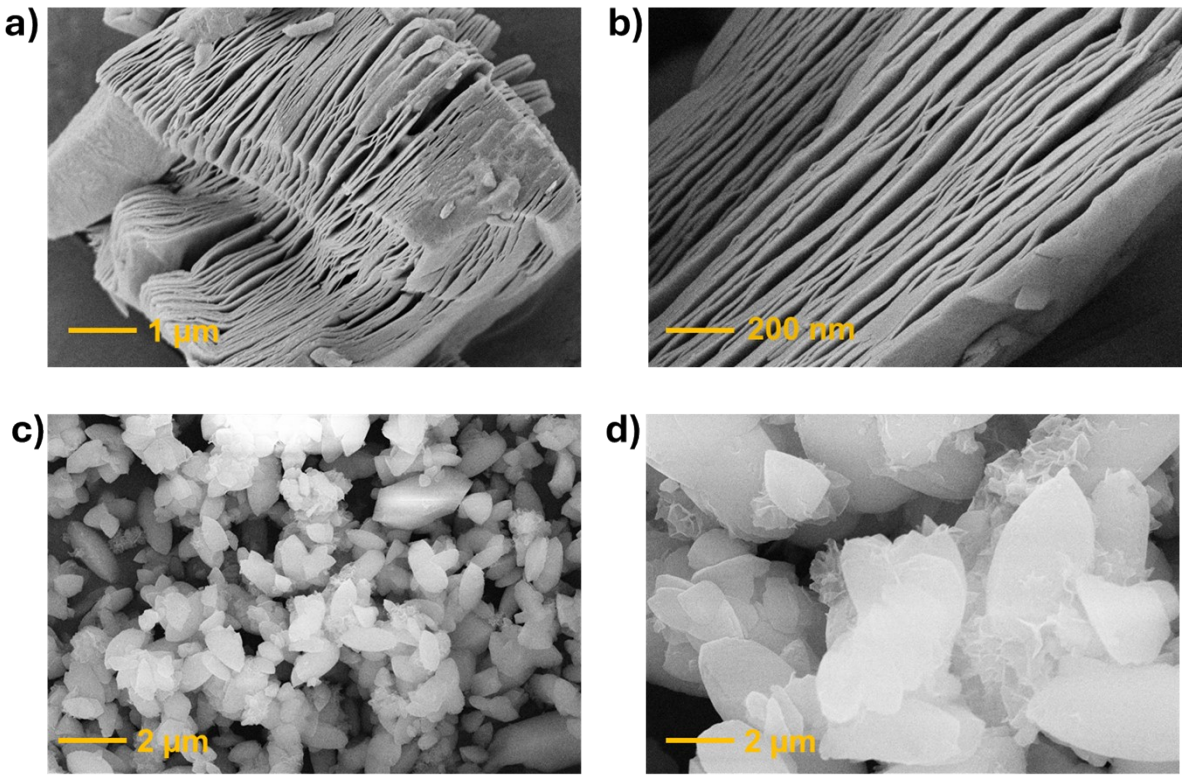

Fig. S3. FE-SEM images of a,b) MXene ($Ti_3C_2T_x$). c,d) Co-MOF at different magnifications respectively.

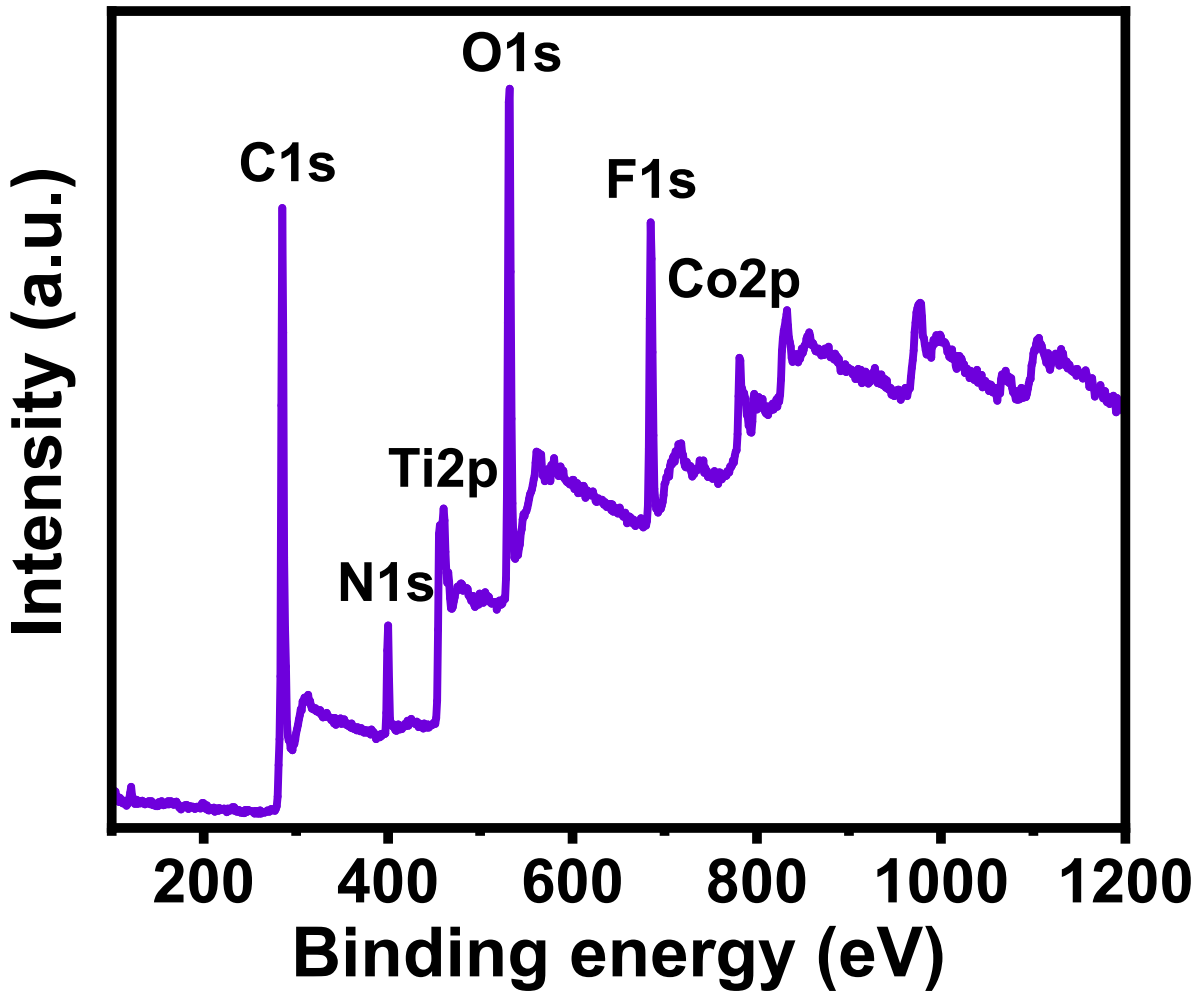

Fig. S4. XPS Survey scan of Co-MOF@MXCNF heterostructure.

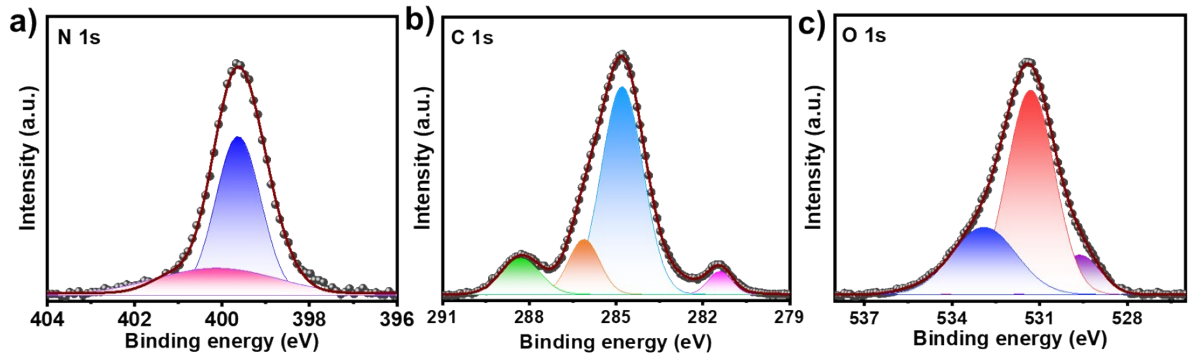

Fig. S5. XPS data of a) N 1s b) C 1s and c) O 1s of Co-MOF@MXCNF.

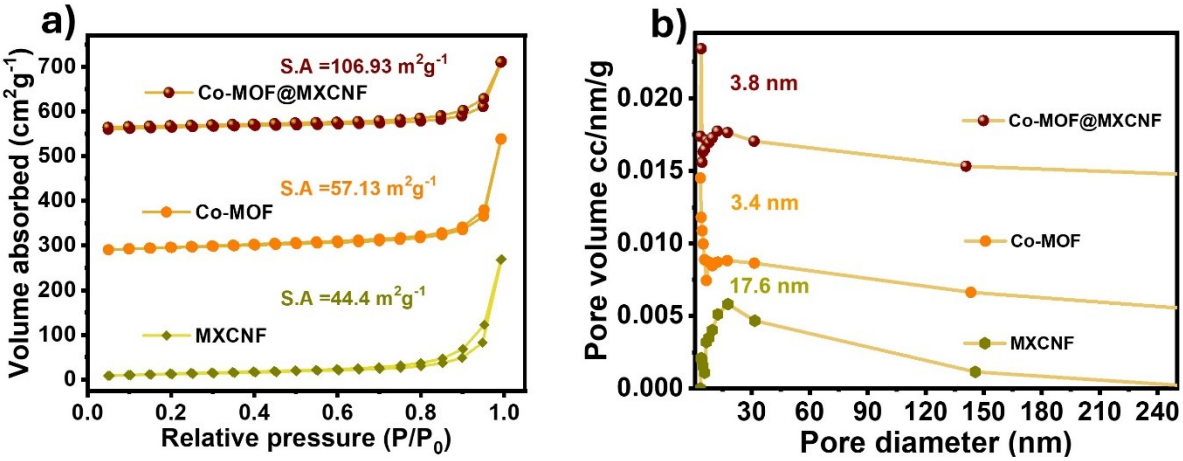

Fig. S6. a) N_2 adsorption and desorption b) BJH pore size distribution of Co-MOF@MXCNF, Co-MOF and MXCNF respectively.

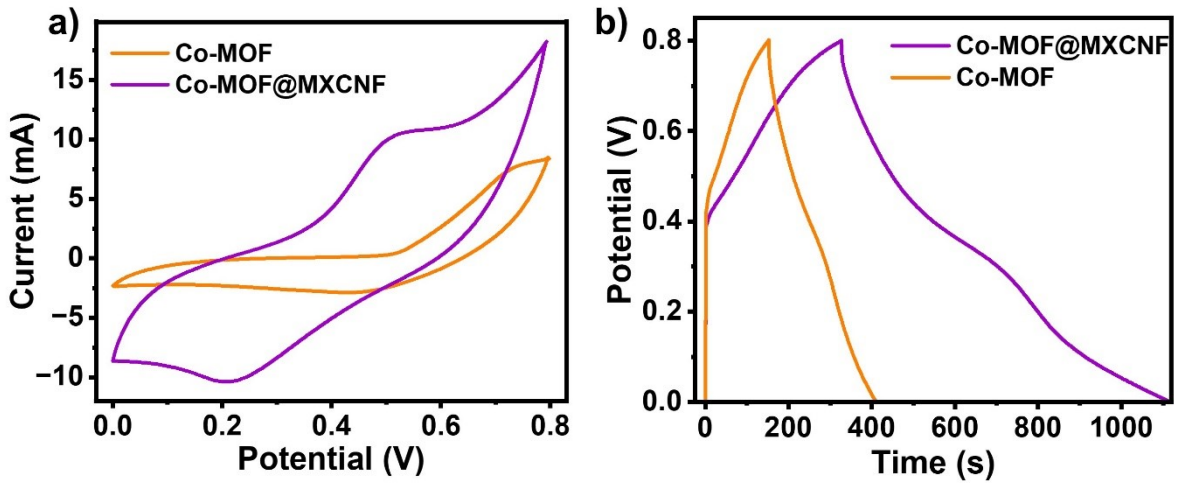

Fig. S7. Electrochemical Performance: (a) Comparison of CV curves of Co-MOF and Co-MOF@MXCNF electrodes measured at a scan rate of 100 mV s^{-1}. (b) Comparison of GCD curves of the Co-MOF and Co-MOF@MXCNF electrode at 1 A g^{-1} current density.

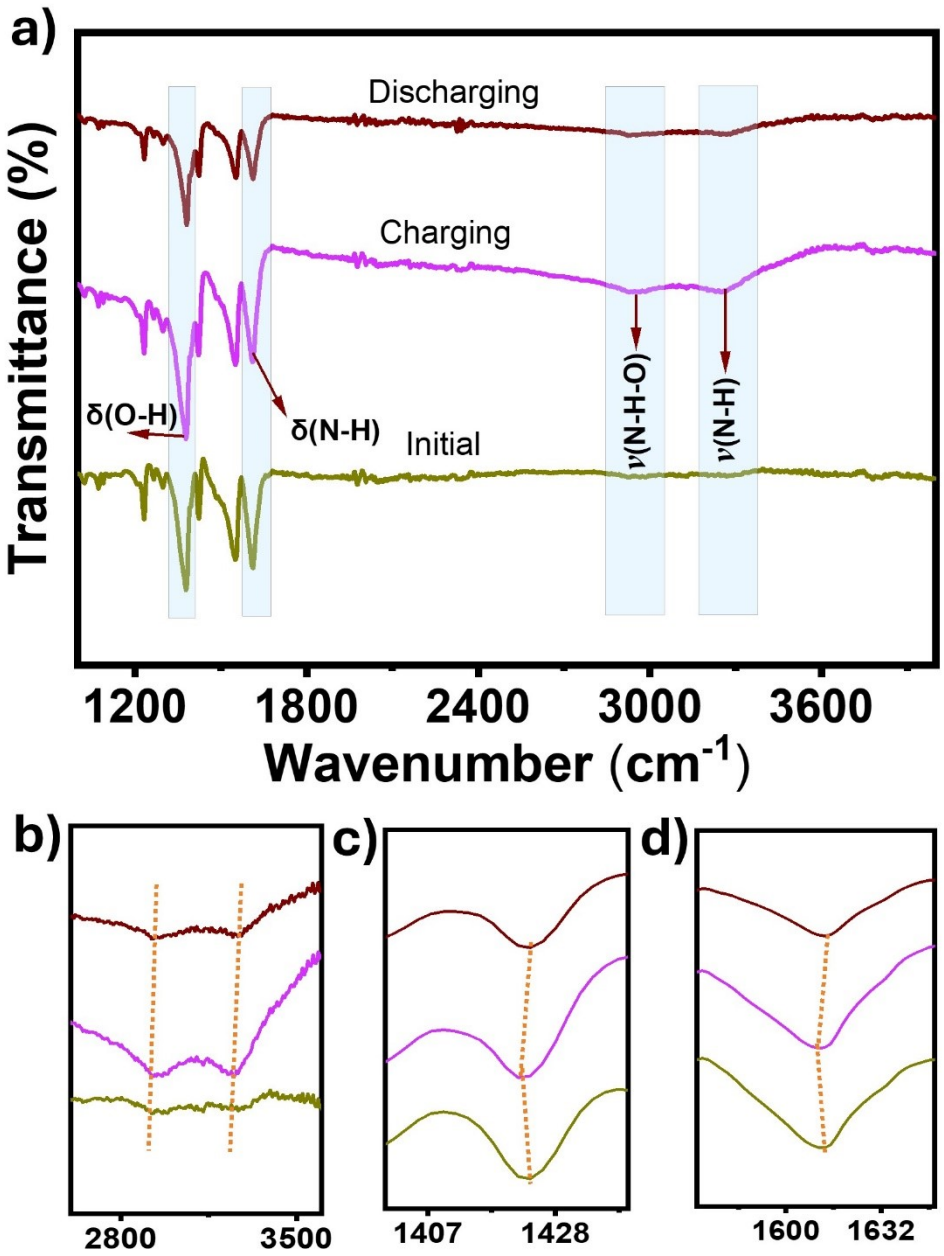

Fig. S8. ATR-FTIR spectrum of Co-MOF@MXCNF for initial, Charging, and discharging respectively.

Table S1: X-ray crystal structure data and refinement parameters of Co-MOF

Parameters	**Co-MOF**
empirical formula	C6 H5 Co0.50 N O3
formula weight	168.57
crystal system	trigonal
space group	*P 31 2 1*
a (Å)	11.9831(6)
b (Å)	11.9593(6)
c (Å)	8.3350(4)
α (deg)	90
β (deg)	90
γ (deg)	120
wavelength (nm)	0.71073
V (Å^3)	1036.51(9)
Z, d_{calcd} (mg m^{-3})	4
temperature (K)	293(2) K
θ range/deg	3.19 to 29.13
goodness-of-fit (GOOF)	1.067
R_1, a wR_2b [I > 2σ(I)]	R1 = 0.0590, wR2 = 0.1274
R_1, *a* wR_2 b (all data)	R1 = 0.0882, wR2 = 0.1459
absorption correction	Semi-empirical from equivalents
refinement method	Full-matrix least-squares on F2
R(int)	0.1567
F (000)	513
CCDC no.	2402755

Table S2: Bond Length and Bond Angle for Co-MOF

Bond Length

Atom 1	Atom 2	Length (Å)
CO01	O007	2.042
	O008	2.063
	O00C	2.071
	O009	2.1
	N00J	2.134
	O003	2.193
CO02	O004	2.045
	O00E	2.081
	O005	2.107
	O00A	2.114
	O00G	2.128
	O003	2.177
O003	CO02	2.177
	CO01	2.193
O004	C00D	1.333
	CO02	2.045
	O008	2.265
	C00F	2.416
	H00U	2.496
O005	C00T	1.249
	CO02	2.107
	O00B	2.254
	C00O	2.368
	H00H	2.487
O006	C00W	1.305
	O009	2.275
	C00I	2.393
O007	C00L	1.242
	CO01	2.042
	O00A	2.17
	C00K	2.36
O008	C00D	1.245
	CO01	2.063
	O004	2.265
	C00F	2.342
	H00V	2.47

	H013	2.475
O009	C00W	1.318
	CO01	2.1
	O006	2.275
	C00I	2.429
O00A	C00L	1.217
	CO02	2.114
	O007	2.17
	C00K	2.337
O00B	C00T	1.323
	O005	2.254
	C00O	2.455
O00C	H00B	0.912
	H00A	0.912
	CO01	2.071
H00A	O00C	0.912
	H00B	1.435
	H00C	2.428
H00B	O00C	0.912
	H00A	1.435
C00D	O008	1.245
	O004	1.333
	C00F	1.477
	C00V	2.446
O00E	H00C	0.857
	H00D	0.857
	CO02	2.081
H00C	O00E	0.857
	H00D	1.355
	H00A	2.428
H00D	O00E	0.857
	H00C	1.355
C00F	C00V	1.306
	C00U	1.442
	C00D	1.477
	H00V	1.925
	H00U	2.061
	O008	2.342
	C00K	2.395
	O004	2.416
	C00N	2.489
O00G	H00E	0.932
	H00F	0.936
	CO02	2.128
H00E	O00G	0.932
	H00F	1.467
H00F	O00G	0.936

	H00E	1.467
	H011	2.077
	C011	2.316
C00H	H00H	0.93
	C00O	1.329
	C00I	1.423
	C00P	2.341
	C00S	2.348
	C00T	2.489
	C00W	2.498
H00H	C00H	0.93
	C00O	1.947
	C00I	2.033
	O005	2.487
C00I	C00S	1.371
	C00H	1.423
	C00W	1.475
	H00S	1.981
	H00H	2.033
	O006	2.393
	C00M	2.426
	O009	2.429
	C00O	2.431
N00J	C012	1.361
	C013	1.381
	H013	1.937
	H012	1.971
	CO01	2.134
	C010	2.416
	C011	2.442
C00K	C00Q	1.373
	C00V	1.402
	C00L	1.504
	H00Q	1.991
	H00V	2.012
	O00A	2.337
	O007	2.36
	C00F	2.395
	C00N	2.445
C00L	O00A	1.217
	O007	1.242
	C00K	1.504
	C00Q	2.496
C00M	C00S	1.366
	C00P	1.387
	C00R	1.559
	H00S	1.976

	H00P	2.01
	H00I	2.081
	H00G	2.081
	C00I	2.426
	C00O	2.452
C00N	C00Q	1.404
	C00U	1.406
	C00R	1.512
	H00Q	2.019
	H00U	2.028
	H00I	2.039
	H00G	2.039
	C00K	2.445
	C00F	2.489
C00O	C00H	1.329
	C00P	1.416
	C00T	1.512
	H00H	1.947
	H00P	2.036
	O005	2.368
	C00I	2.431
	C00M	2.452
	O00B	2.455
C00P	H00P	0.93
	C00M	1.387
	C00O	1.416
	C00S	2.336
	C00H	2.341
H00P	C00P	0.93
	C00M	2.01
	C00O	2.036
C00Q	H00Q	0.93
	C00K	1.373
	C00N	1.404
	C00V	2.369
	C00U	2.377
	C00L	2.496
H00Q	C00Q	0.93
	C00K	1.991
	C00N	2.019
	H00I	2.413
C00R	H00I	0.97
	H00G	0.97
	C00N	1.512
	C00M	1.559
H00G	C00R	0.97
	H00I	1.565

	C00N	2.039
	C00M	2.081
H00I	C00R	0.97
	H00G	1.565
	C00N	2.039
	C00M	2.081
	H00Q	2.413
C00S	H00S	0.93
	C00M	1.366
	C00I	1.371
	C00P	2.336
	C00H	2.348
H00S	C00S	0.93
	C00M	1.976
	C00I	1.981
C00T	O005	1.249
	O00B	1.323
	C00O	1.512
	C00H	2.489
C00U	H00U	0.93
	C00N	1.406
	C00F	1.442
	C00V	2.352
	C00Q	2.377
H00U	C00U	0.93
	C00N	2.028
	C00F	2.061
	O004	2.496
C00V	H00V	0.93
	C00F	1.306
	C00K	1.402
	C00U	2.352
	C00Q	2.369
	C00D	2.446
H00V	C00V	0.93
	C00F	1.925
	C00K	2.012
	O008	2.47
C00W	O006	1.305
	O009	1.318
	C00I	1.475
	C00H	2.498
C00Z	C011	1.412
	C00Z	1.46
	C010	1.561
	H011	2.04
	H010	2.208

	C013	2.354
	C012	2.434
C010	H010	0.93
	C013	1.23
	C00Z	1.561
	H013	1.802
	N00J	2.416
	C011	2.495
H010	C010	0.93
	C013	1.902
	H013	2.089
	C00Z	2.208
	H011	2.27
C011	H011	0.93
	C012	1.391
	C00Z	1.412
	H012	1.999
	H00F	2.316
	N00J	2.442
	C010	2.495
H011	C011	0.93
	C012	2.021
	C00Z	2.04
	H00F	2.077
	H010	2.27
	H012	2.282
C012	H012	0.93
	N00J	1.361
	C011	1.391
	H011	2.021
	C013	2.255
	C00Z	2.434
H012	C012	0.93
	N00J	1.971
	C011	1.999
	H011	2.282
C013	H013	0.93
	C010	1.23
	N00J	1.381
	H010	1.902
	C012	2.255
	C00Z	2.354
H013	C013	0.93
	C010	1.802
	N00J	1.937
	H010	2.089
	O008	2.475

Bond Angles

Atom1	Atom2	Atom3	Angle
O007	CO01	O00C	174.4
O007	CO01	N00J	89.72
O007	CO01	O009	85.99
O007	CO01	O003	89.63
O007	CO01	O008	97.28
O00C	CO01	N00J	88.28
O00C	CO01	O009	88.85
O00C	CO01	O003	92.37
O00C	CO01	O008	87.87
N00J	CO01	O009	92.07
N00J	CO01	O003	179.35
N00J	CO01	O008	87.61
O009	CO01	O003	87.93
O009	CO01	O008	176.71
O003	CO01	O008	92.42
O003	CO02	O004	91.86
O003	CO02	O00E	93.17
O003	CO02	O00G	176.07
O003	CO02	O005	88.51
O003	CO02	O00A	90.96
O004	CO02	O00E	170.52
O004	CO02	O00G	85.43
O004	CO02	O005	88.5
O004	CO02	O00A	101.54
O00E	CO02	O00G	89.11
O00E	CO02	O005	83.6
O00E	CO02	O00A	86.42
O00G	CO02	O005	88.56
O00G	CO02	O00A	92.38
O005	CO02	O00A	169.96
CO02	O003	CO01	112.25
CO02	O004	C00D	135.95
C00T	O005	CO02	129.08
CO01	O007	C00L	137.99
C00D	O008	CO01	139.55
C00W	O009	CO01	129.23

C00L	O00A	CO02	133.37
CO01	O00C	H00A	128.43
CO01	O00C	H00B	127.84
H00A	O00C	H00B	103.73
O004	C00D	O008	122.83
O004	C00D	C00F	118.43
O008	C00D	C00F	118.41
CO02	O00E	H00C	126.85
CO02	O00E	H00D	128.67
H00C	O00E	H00D	104.44
C00D	C00F	C00U	119.45
C00D	C00F	C00V	122.91
C00U	C00F	C00V	117.63
CO02	O00G	H00E	126.7
CO02	O00G	H00F	129.76
H00E	O00G	H00F	103.53
H00H	C00H	C00I	117.97
H00H	C00H	C00O	117.97
C00I	C00H	C00O	124.07
C00H	C00I	C00S	114.36
C00H	C00I	C00W	119.08
C00S	C00I	C00W	125.88
CO01	N00J	C012	124.32
CO01	N00J	C013	124.89
C012	N00J	C013	110.59
C00L	C00K	C00Q	120.27
C00L	C00K	C00V	122.45
C00Q	C00K	C00V	117.25
O007	C00L	O00A	123.8
O007	C00L	C00K	118.22
O00A	C00L	C00K	117.98
C00P	C00M	C00R	121.65
C00P	C00M	C00S	116.09
C00R	C00M	C00S	121.73
C00Q	C00N	C00R	122.22
C00Q	C00N	C00U	115.5
C00R	C00N	C00U	121.95
C00H	C00O	C00P	117.08
C00H	C00O	C00T	122.21
C00P	C00O	C00T	120.72
C00M	C00P	C00O	122.02
C00M	C00P	H00P	118.99
C00O	C00P	H00P	118.99
C00K	C00Q	C00N	123.37
C00K	C00Q	H00Q	118.32
C00N	C00Q	H00Q	118.32
C00M	C00R	C00N	115.1

C00M	C00R	H00G	108.5
C00M	C00R	H00I	108.5
C00N	C00R	H00G	108.5
C00N	C00R	H00I	108.5
H00G	C00R	H00I	107.51
C00I	C00S	C00M	124.87
C00I	C00S	H00S	117.56
C00M	C00S	H00S	117.56
O005	C00T	O00B	122.37
O005	C00T	C00O	117.8
O00B	C00T	C00O	119.77
C00F	C00U	C00N	121.81
C00F	C00U	H00U	119.09
C00N	C00U	H00U	119.09
C00F	C00V	C00K	124.31
C00F	C00V	H00V	117.84
C00K	C00V	H00V	117.84
O006	C00W	O009	120.25
O006	C00W	C00I	118.62
O009	C00W	C00I	120.7
C010	C00Z	C011	114.02
C010	C00Z	C00Z	121.38
C011	C00Z	C00Z	124.37
C00Z	C010	H010	122.79
C00Z	C010	C013	114.42
H010	C010	C013	122.79
C00Z	C011	H011	119.72
C00Z	C011	C012	120.57
H011	C011	C012	119.72
N00J	C012	C011	125.05
N00J	C012	H012	117.48
C011	C012	H012	117.48
N00J	C013	C010	135.27
N00J	C013	H013	112.36
C010	C013	H013	112.36
C012	N00J	C013	110.59
C012	N00J	CO01	124.32
C013	N00J	CO01	124.89
C00Z	C00Z	C010	121.38
C00Z	C00Z	C011	124.37
C010	C00Z	C011	114.02
C00Z	C010	H010	122.79
C00Z	C010	C013	114.42
H010	C010	C013	122.79
C00Z	C011	H011	119.72
C00Z	C011	C012	120.57
H011	C011	C012	119.72

N00J	C012	C011	125.05
N00J	C012	H012	117.48
C011	C012	H012	117.48
N00J	C013	C010	135.27
N00J	C013	H013	112.36
C010	C013	H013	112.36
O009	CO01	O007	85.99
O009	CO01	O00C	88.85
O009	CO01	O003	87.93
O009	CO01	O008	176.71
O009	CO01	N00J	92.07
O007	CO01	O00C	174.4
O007	CO01	O003	89.63
O007	CO01	O008	97.28
O007	CO01	N00J	89.72
O00C	CO01	O003	92.37
O00C	CO01	O008	87.87
O00C	CO01	N00J	88.28
O003	CO01	O008	92.42
O003	CO01	N00J	179.35
O008	CO01	N00J	87.61
O003	CO02	O004	91.86
O003	CO02	O00E	93.17
O003	CO02	O00G	176.07
O003	CO02	O005	88.51
O003	CO02	O00A	90.96
O004	CO02	O00E	170.52
O004	CO02	O00G	85.43
O004	CO02	O005	88.5
O004	CO02	O00A	101.54
O00E	CO02	O00G	89.11
O00E	CO02	O005	83.6
O00E	CO02	O00A	86.42
O00G	CO02	O005	88.56
O00G	CO02	O00A	92.38
O005	CO02	O00A	169.96
CO02	O003	CO01	112.25
CO02	O004	C00D	135.95
C00T	O005	CO02	129.08
CO01	O007	C00L	137.99
C00D	O008	CO01	139.55
CO01	O009	C00W	129.23
C00L	O00A	CO02	133.37
CO01	O00C	H00A	128.43
CO01	O00C	H00B	127.84
H00A	O00C	H00B	103.73
O004	C00D	O008	122.83

O004	C00D	C00F	118.43
O008	C00D	C00F	118.41
CO02	O00E	H00C	126.85
CO02	O00E	H00D	128.67
H00C	O00E	H00D	104.44
C00D	C00F	C00U	119.45
C00D	C00F	C00V	122.91
C00U	C00F	C00V	117.63
CO02	O00G	H00E	126.7
CO02	O00G	H00F	129.76
H00E	O00G	H00F	103.53
H00H	C00H	C00I	117.97
H00H	C00H	C00O	117.97
C00I	C00H	C00O	124.07
C00H	C00I	C00S	114.36
C00H	C00I	C00W	119.08
C00S	C00I	C00W	125.88
C00L	C00K	C00Q	120.27
C00L	C00K	C00V	122.45
C00Q	C00K	C00V	117.25
O007	C00L	O00A	123.8
O007	C00L	C00K	118.22
O00A	C00L	C00K	117.98
C00P	C00M	C00R	121.65
C00P	C00M	C00S	116.09
C00R	C00M	C00S	121.73
C00Q	C00N	C00R	122.22
C00Q	C00N	C00U	115.5
C00R	C00N	C00U	121.95
C00H	C00O	C00P	117.08
C00H	C00O	C00T	122.21
C00P	C00O	C00T	120.72
C00M	C00P	C00O	122.02
C00M	C00P	H00P	118.99
C00O	C00P	H00P	118.99
C00K	C00Q	C00N	123.37
C00K	C00Q	H00Q	118.32
C00N	C00Q	H00Q	118.32
C00M	C00R	C00N	115.1
C00M	C00R	H00G	108.5
C00M	C00R	H00I	108.5
C00N	C00R	H00G	108.5
C00N	C00R	H00I	108.5
H00G	C00R	H00I	107.51
C00I	C00S	C00M	124.87
C00I	C00S	H00S	117.56
C00M	C00S	H00S	117.56

O005	C00T	O00B	122.37
O005	C00T	C00O	117.8
O00B	C00T	C00O	119.77
C00F	C00U	C00N	121.81
C00F	C00U	H00U	119.09
C00N	C00U	H00U	119.09
C00F	C00V	C00K	124.31
C00F	C00V	H00V	117.84
C00K	C00V	H00V	117.84
O006	C00W	O009	120.25
O006	C00W	C00I	118.62
O009	C00W	C00I	120.7
O003	CO01	O008	92.42
O003	CO01	O008	92.42
O00A	CO02	O003	90.96
O00A	CO02	O003	90.96
CO01	O003	CO02	112.25
CO01	O003	CO02	112.25

Table S3. Comparison of as-synthesized material with previous reports.

S. No.	Material	Capacitance ($F\ g^{-1}$/ $F\ cm^{-2}$) at Current density ($A\ g^{-1}$ or $F\ cm^{-2}$)	Electrolyte	Ref.
1	Cu-HHB/I_2	111.7 mF cm^{-2} at 0.4 mA cm^{-2}	1 M $(NH_4)_2SO_4$	[3]
2	PMO	15.3 F cm^{-2} at 2 mA cm^{-2}	2 M NH_4Ac	[4]
3	δ-MnO_2	9.5 F cm^{-2} at 2 mA cm^{-2}	1 M $(NH_4)_2SO_4$	[5]
4	(NH4)$x$$WO_3$	8.0 F cm^{-2} at 2 mA cm^{-2}	2 M NH_4Ac	[6]
5	$(NH_4)_2V_{10}O_{25}\cdot 8H_2O$	339 F g^{-1} at 0.5 A g^{-1}	NH_4Cl/PVA electrolyte	[7]
7	MoS_2@PANI	452 F g^{-1} 1 A g^{-1}	1 M NH_4Cl	[8]
8	MoO_3@C	473 F·g^{-1} at 1 A·g^{-1}	1 $(NH4)_2SO_4$	[9]
9	MnO_x	176 mAh g^{-1} at 0.5 A g^{-1}	0.5 M NH_4Ac	[10]
10	HPCNFs@Ni-BTA	678.5 F g^{-1} at 0.5 A g^{-1}	1 M NH_4Ac	[11]
11	MoS_2@TiN/CNTF	1102.5 mF cm^{-2} at 2 mA cm^{-2}	1.0 M NH_4Cl	[12]
12	h-Ti3C2 MXene	274.25 F g^{-1} at 1 A g^{-1}	1 M NH_4Ac	[13]
13	**Co-MOF@MXCNF**	**980 F g^{-1} at 1 A g^{-1}**	**2 M $(NH4)_2SO_4$**	**This work**

Table S4. Comparison of as-synthesized material with previous AIHSCs reports

S. No.	Materials	Energy density (E_d)	Power density (P_d)	Electrolytes	References
1	δ-MnO2//ACC	861.2	20.0	1 M $(NH_4)_2SO_4$	[14]
2	α-MnO2//(NH4)xWO3	1010.1	18.0	2 M NH_4Ac	[15]
3	MnO2/CNTF//MoS2@TiN/CNTF	195.1	1.1	PVA/NH_4Cl	[16]
4	ACC@VPP//PTCDI	320	0.09	PVA/NH_4Cl	[17]
5	Cu-HHB/I2//P-MXene	31.5 mWh cm-2	400	1 M $(NH_4)_2SO_4$	[18]
6	PMO//MnO2	2.48 Wh cm−2	20.0 mW cm−2	2.0 M NH_4Ac	[19]
7	MnO_2@ACC//WO_3@ACC	508.1 μW h cm^{-2}	1.8 mW cm^{-2}	NH_4Cl/PVA	[20]
8	h-Ti3C2 Mxene// MnO2 CNTs	394.59 μWh cm^{-2}	16.50 mW cm^{-2}	PAM hydrogel electrolyte	[13]
9	**Co-MOF@MXCNF//MXCNF**	**41.2 mWh kg^{-1}**	**799.6 mW kg^{-1}**	**1 M $(NH_4)_2SO_4$ /PVA**	**This work**

References

1 G. M. Sheldrick, *Acta Cryst A*, 2008, **64**, 112–122.

2 G. Bergerhoff, M. Berndt and K. Brandenburg, *J Res Natl Inst Stand Technol*, 1996, **101**, 221–225.

3 M. Gao, Z. Wang, Z. Liu, Y. Huang, F. Wang, M. Wang, S. Yang, J. Li, J. Liu, H. Qi, P. Zhang, X. Lu and X. Feng, *Advanced Materials*, 2023, **35**, 2305575.

4 Q. Chen, H. Li, X. Lou, J. Zhang, G. Hou, J. Lu and Y. Tang, *Advanced Functional Materials*, 2023, **33**, 2214920.

5 Q. Chen, J. Jin, M. Song, X. Zhang, H. Li, J. Zhang, G. Hou, Y. Tang, L. Mai and L. Zhou, *Advanced Materials*, 2022, **34**, 2107992.

6 Q. Chen, M. Song, X. Zhang, J. Zhang, G. Hou and Y. Tang, *J. Mater. Chem. A*, 2022, **10**, 15614–15622.

7 P. Wang, Y. Zhang, H. Jiang, X. Dong and C. Meng, *Chemical Engineering Journal*, 2022, **427**, 131548.

8 J. Dai, C. Yang, Y. Xu, X. Wang, S. Yang, D. Li, L. Luo, L. Xia, J. Li, X. Qi, A. Cabot and L. Dai, *Adv Mater*, 2023, **35**, e2303732.

9 J. Dai, X. Qi, L. Xia, Q. Xue, L. Luo, X. Wang, C. Yang, D. Li, H. Xie, A. Cabot, L. Dai and Y. Xu, *Advanced Functional Materials*, 2023, **33**, 2212440.

10 Y. Song, Q. Pan, H. Lv, D. Yang, Z. Qin, M.-Y. Zhang, X. Sun and X.-X. Liu, *Angew Chem Int Ed Engl*, 2021, **60**, 5718–5722.

11 Y. Huang, M. Gao, Y. Fu, J. Li, F. Wang, S. Yang, M. Wang, Z. Qian, X. Lu, P. Zhang and R. Wang, *Energy Storage Materials*, 2024, **70**, 103522.

12 L. Han, J. Luo, R. Zhang, W. Gong, L. Chen, F. Liu, Y. Ling, Y. Dong, Z. Yong, Y. Zhang, L. Wei, X. Zhang, Q. Zhang and Q. Li, *ACS Nano*, 2022, **16**, 14951–14962.

13 J. Shi, K. Niu, L. Zhang, Q. Chen, M. Deng, L. Sun, S. Cheng and Y. Gao, *ACS Energy Lett.*, 2024, **9**, 2000–2006.

14 Q. Chen, J. Jin, M. Song, X. Zhang, H. Li, J. Zhang, G. Hou, Y. Tang, L. Mai and L. Zhou, *Advanced Materials*, 2022, **34**, 2107992.

15 Q. Chen, M. Song, X. Zhang, J. Zhang, G. Hou and Y. Tang, *J. Mater. Chem. A*, 2022, **10**, 15614–15622.

16 L. Han, J. Luo, R. Zhang, W. Gong, L. Chen, F. Liu, Y. Ling, Y. Dong, Z. Yong, Y. Zhang, L. Wei, X. Zhang, Q. Zhang and Q. Li, *ACS Nano*, 2022, **16**, 14951–14962.

17 X. Chen, P. Wang, Z. Feng, C. Meng and Y. Zhang, *Chemical Engineering Journal*, 2022, **445**, 136747.

18 M. Gao, Z. Wang, Z. Liu, Y. Huang, F. Wang, M. Wang, S. Yang, J. Li, J. Liu, H. Qi, P. Zhang, X. Lu and X. Feng, *Advanced Materials*, 2023, **35**, 2305575.

19 C. Qiang, H. Li, X. Lou, J. Zhang, G.-Y. Hou, J. Lu and Y. Tang, *Advanced Functional Materials*, DOI:10.1002/adfm.202214920.

20 Z. Han, X. Zhang, G. Tang, J. Liang and W. Wu, *Journal of Energy Storage*, 2024, **91**, 112023.